0090-9556/07/3510-1766–1780$20.00
DRUG METABOLISM AND DISPOSITION
Vol. 35, No. 10
15644/3252832
DMD 35:1766–1780, 2007
Printed in U.S.A.

Prediction of Human Pharmacokinetics Using Physiologically Based Modeling: A Retrospective Analysis of 26 Clinically Tested Drugs

Stefan S. De Buck, Vikash K. Sinha, Luca A. Fenu, Marjoleen J. Nijsen, Claire E. Mackie, and Ron A. H. J. Gilissen

Johnson & Johnson Pharmaceutical Research and Development, Discovery ADME-Tox Department, Beerse, Belgium

Received March 5, 2007; accepted July 3, 2007

ABSTRACT:

The aim of this study was to evaluate different physiologically based modeling strategies for the prediction of human pharmacokinetics. Plasma profiles after intravenous and oral dosing were simulated for 26 clinically tested drugs. Two mechanism-based predictions of human tissue-to-plasma partitioning (P_{tp}) from physicochemical input (method Vd1) were evaluated for their ability to describe human volume of distribution at steady state (V_{ss}). This method was compared with a strategy that combined predicted and experimentally determined in vivo rat P_{tp} data (method Vd2). Best V_{ss} predictions were obtained using method Vd2, providing that rat P_{tp} input was corrected for interspecies differences in plasma protein binding (84% within 2-fold). V_{ss} predictions from physicochemical input alone were poor (32% within 2-fold). Total body clearance (CL) was predicted as the sum of scaled rat renal clearance and hepatic clearance projected from in vitro metabolism data. Best CL predictions were obtained by disregarding both blood and microsomal or hepatocyte binding (method CL2, 74% within 2-fold), whereas strong bias was seen using both blood and microsomal or hepatocyte binding (method CL1, 53% within 2-fold). The physiologically based pharmacokinetics (PBPK) model, which combined methods Vd2 and CL2 yielded the most accurate predictions of in vivo terminal half-life (69% within 2-fold). The Gastroplus advanced compartmental absorption and transit model was used to construct an absorption-disposition model and provided accurate predictions of area under the plasma concentration-time profile, oral apparent volume of distribution, and maximum plasma concentration after oral dosing, with 74%, 70%, and 65% within 2-fold, respectively. This evaluation demonstrates that PBPK models can lead to reasonable predictions of human pharmacokinetics.

In the drug discovery process considerable resources are required to assess the pharmacokinetic (PK) properties of potential drug candidates in vivo in animals. To optimize the use of such in vivo testing, there has been a growing interest in predicting the PK behavior of drug candidates (Theil et al., 2003; van de Waterbeemd and Gifford, 2003). If sufficiently reliable, such simulations could also help to select the most promising candidates for development and reject those with a low probability of success (van de Waterbeemd and Gifford, 2003).

The majority of the approaches to predict human PK developed to date typically focus on the drug's behavior in individual processes of absorption, distribution, metabolism and excretion (ADME). The characterization of a drug's PK in a complex biological system is best described by assembling these processes in one global model. In this context, physiologically based pharmacokinetics (PBPK) models have been developed (Bischoff, 1986). PBPK models map the complex drug transport scheme onto a physiologically realistic compartmental structure (Fig. 1). The major structural elements of the PBPK disposition model are derived from the anatomical structure of the organism; therefore, the model structure is predetermined and basically independent of the drug of interest. The PBPK model input parameters include both a drug-independent and a drug-specific subset. The first subset comprises data underlying the physiological processes (e.g., blood flow), and the second subset comprises drug-specific biochem-

Article, publication date, and citation information can be found at http://dmd.aspetjournals.org.
doi:10.1124/dmd.107.015644.

ABBREVIATIONS: PK, pharmacokinetic(s); ACAT, advanced compartmental absorption and transit model; ADME, absorption, distribution, metabolism, and excretion; AUC, area under the plasma concentration-time curve; AUMC, area under the first moment curve; BCS, Biopharmaceutical Classification Scheme; CL, total body clearance from plasma; CL/*F*, total body clearance from plasma after oral administration; CL_H, hepatic plasma clearance; $CL_{H,blood}$, hepatic blood clearance; CL_{int}, intrinsic clearance; CL_R, renal clearance from plasma; C_{max}, peak plasma concentration after oral administration; *D*, dose; *F*, absolute oral bioavailability; fu_{inc}, unbound fraction in microsomal or hepatocyte incubation; fu_p, unbound fraction in plasma; GFR, glomerular filtration rate; in vivo $t_{1/2}$, in vivo terminal half-life; log P_{ow}, *n*-octanol:water partition coefficient of the non-ionized species; PBPK, physiologically based pharmacokinetics; P_{tp}, tissue-to-plasma partition coefficient; P_{tpu}, tissue-to-plasma partition coefficient of the unbound drug; Q_h, hepatic blood flow; RA, ratio of albumin concentration found in tissue over plasma; R_B, blood-to-plasma concentration ratio; SF, scaling factor; SIF, simulated intestinal fluid; V_d/F, apparent volume of distribution after oral administration; V_{ss}, apparent volume of distribution at steady state.

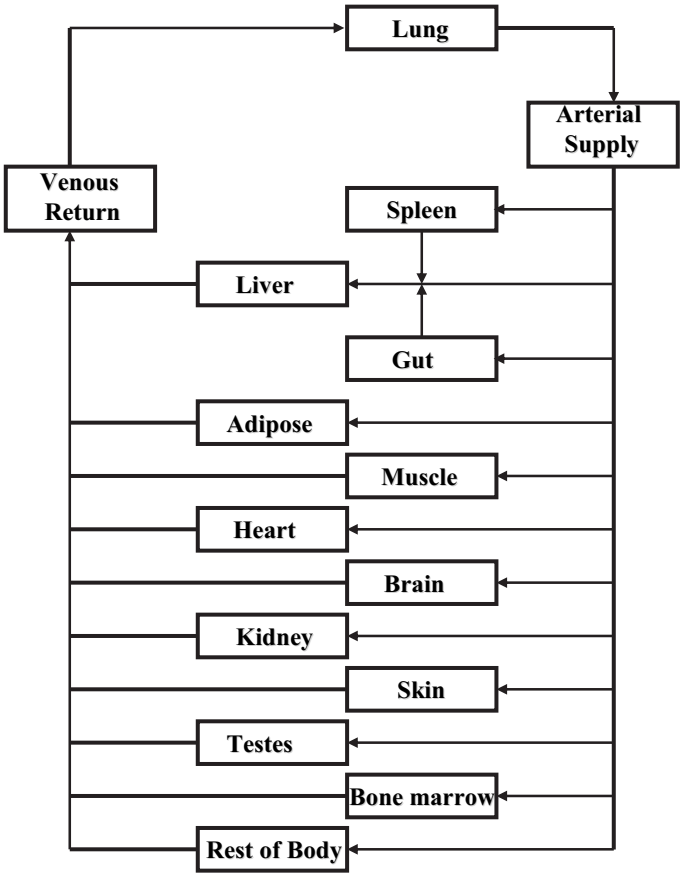

FIG. 1. Scheme of the generic disposition PBPK model for simulation of full plasma and tissue concentration-time profiles in rat and human. An overview of all physiological values is given in Table 3. Estimation of rate and extent of oral absorption from the gut was obtained using ACAT (Yu and Amidon, 1999; Agoram et al., 2001). For more details on all methods used, refer to *Materials and Methods*.

ical parameters. The latter consists of the drug's in vivo intrinsic clearance (CL_{int}) of each organ involved in its elimination, in addition to estimates of the drug's tissue-to-plasma coefficient (P_{tp}) for each model compartment. Prediction of the rate and extent of absorption can be obtained using semiphysiologically based absorption models, such as the advanced compartmental absorption and transit (ACAT) model (Yu and Amidon, 1999; Agoram et al., 2001). As depicted in Fig. 1, the ACAT model may serve as a time-dependent input function to the disposition model, thereby creating a combined absorption-distribution PBPK model.

Although PBPK models have been widely used in areas such as risk assessment to predict the PK behavior of toxic chemicals, their application in support of drug discovery and development has remained limited, most probably as a result of their mathematical complexity and the labor-intensive drug-specific input data required. However, more recently, a variety of in vitro based prediction tools have been developed for the estimation of PBPK model input parameters (Theil et al., 2003). Such prediction tools require commonly determined biochemical and physicochemical drug-specific input and thus allow for the prediction of ADME parameters before any in vivo experiment. As examples of such prediction tools, mechanistic equations have been developed for the prediction of fraction of oral dose absorbed (Agoram et al., 2001; Willmann et al., 2004), tissue partitioning (P_{tp}) (Poulin and Theil, 2000; Poulin et al., 2001; Rodgers et al., 2005a), apparent volume of distribution at steady state (V_{ss}) (Poulin and Theil, 2002), and hepatic plasma clearance (CL_H) (Houston and Carlile, 1997; Austin et al., 2002; Ito and Houston, 2004). In a previous study, we also evaluated a variety of physiologically based prediction tools for the prediction of rat PK (De Buck et al., 2007).

The aim of the present work was to further evaluate these prediction tools for their ability to predict human PK parameters by simulation of full plasma concentration-time profiles after both intravenous and oral administration. Although recent studies have addressed a similar question, the overall prediction accuracy obtained was in the lower range, particularly for predictions of V_{ss} and in vivo terminal half-life (in vivo $t_{1/2}$) (Parrott et al., 2005b; Jones et al., 2006a). In the present study, a more comprehensive range of approaches toward the prediction of V_{ss} and CL_H was explored, including two mechanism-based V_{ss} predictions from physicochemical input, as well as approaches that combine the use of both predicted and experimentally determined in vivo rat P_{tp}. For each of the approaches tested, the influence of interspecies differences in plasma protein binding on prediction accuracy was investigated. The role of relative drug binding in plasma and in vitro drug matrices was also considered with respect to CL_H projection from in vitro metabolism data. Whereas the basic tenet of pharmacokinetics states that the unbound drug concentration in the plasma dictates clearance, our previous report in rat using microsomes has suggested that in vitro CL_{int} may provide a better estimate of in vivo CL_H of total rather than unbound drug (De Buck et al., 2007). To further investigate the effect of relative drug binding, predictions of human CL_H were performed each time under two variations, either by incorporating or disregarding such binding factors. Methods to predict V_{ss} and CL were combined to predict in vivo $t_{1/2}$, and the ACAT model was tested for its ability to predict the area under the oral concentration-time profile (AUC), the oral apparent volume of distribution (V_d/F), and peak plasma concentration (C_{max}). To determine whether a successful prediction in rat correlates with a successful prediction in human, the accuracy of each method was assessed within both species.

Materials and Methods

Compounds and Sources of in Vitro and in Vivo Parameters. The set of compounds ($n = 26$) included in this analysis were taken from those brought into clinical development at Johnson & Johnson Pharmaceutical Research and Development (Beerse, Belgium). Compounds were selected based on the availability of historical data on the in vivo preclinical (rat) and clinical PK, as well as of each of the following experimentally determined biochemical and physicochemical parameters: unbound fraction in plasma (fu_p), unbound fraction in microsomal or hepatocyte incubation (fu_{inc}), basic and acidic dissociation constants (pK_a), *n*-octanol:water partition coefficient of the non-ionized species ($\log P_{ow}$), aqueous solubility at defined pH conditions or solubility in simulated intestinal fluid (SIF), in vitro CL_{int} determined in hepatic microsomes or hepatocyte suspension cultures, and the blood-to-plasma concentration ratio (R_B). Summaries of the available in vitro and in vivo PK data are shown in Tables 1 and 2, respectively.

The 26 compounds in the data set cover a broad range of small molecules from a variety of discovery programs. The majority of compounds ($n = 19$) were moderate-to-strong bases (pK_a of protonated base >7.0); three were neutral or weakly ionized at physiological pH (weak base). The remaining compounds were one weak acid, one strong acid, and two zwitterions. The lipophilicity ($\log P_{ow}$) ranged between 1.11 and 5.5, and fu_p ranged from 0.001 to 0.867. Aqueous solubility was highly variable with values at physiological pH ranging from 0.003 mg/ml to 74 mg/ml. V_{ss} in humans varied from limited (30 L) to widespread (>1000 L). In the rat, major elimination pathways included hepatic metabolism, renal excretion, or a combination of the two. In humans, total body clearance from plasma (CL) varied from less than 10% of hepatic blood flow (Q_h) to more than 70% of Q_h.

Model Structure. The Gastroplus 5.1.0 generic PBPK model and its built-in mass balance differential equations were used for all simulations (Simulations Plus Inc., Lancaster, CA). In brief, the model (Fig. 1) was composed of 14 tissue compartments, including lung, spleen, liver, gut, adipose tissue, muscle, heart, brain, kidney, skin, testes, red marrow, yellow

TABLE 1

In vitro and in silico physicochemical and biochemical properties of the 26 compounds

JNJ No.	Generic Name	mol. wt.	pK_a	Log P_{ow}	Species	fu_p	fu_{inc}[a]	R_B	In Vivo CL_{int}[b]	Test System	P_{eff}[c,d]	Solubility
									ml/min/kg		*10^{-4} cm/s*	*mg/ml*
JNJ1	Lorcainide	407	B 9.44	4.16	Rat	0.260		1.2	624	RLMic	4.78	265, 214, 192, 2.4, 0.18 in aqueous buffer at pH 2.2, 4.2, 5.9, 7.7 and 9.5, respectively
					Human	0.150	0.45	0.70	31.5	HLMic		
JNJ2	Domperidone	425	B 7.89 B 2.50	3.96	Rat	0.092		1.3	178	RLMic	1.88	0.31, 1.5, 0.057, 0.006, 0.001 in aqueous buffer at pH 2.3, 4.2, 6.0, 7.2, and 8.0, respectively
					Human	0.061	0.34	0.74	69.3	HLMic		
JNJ3	Nebivolol	405	B 8.40	4.03	Rat	0.015		1.2	89.1	RLMic	1.86	0.046, 0.071, 0.91, 0.031, 0.12 in aqueous buffer at pH 1.9, 4.0, 5.4, 6.1, and 8.1, respectively
					Human	0.020	0.12[e]	1.2	11.2	HLMic		
JNJ4	Galantamine	287	B 8.20	1.11	Rat	0.755		1.0	20.8	RLMic	5.43	35, 39, 33, 38, 37, 41 in aqueous buffer at pH 2.0, 4.9, 5.2, 6.8, 7.5, and 7.7, respectively
					Human	0.822	0.86[e]	1.2	2.49	HLMic		
JNJ5	Alfentanil	416	B 6.50	2.21	Rat	0.164		0.69	416	RLMic		
					Human	0.079	0.97	0.63	190	HLMic		
JNJ6	Sufentanil	386	B 8.10	4.02	Rat	0.069		0.74	250	RLMic		
					Human	0.075	0.87	0.74	184	HLMic		
JNJ7	Ketanserin	395	B 7.50	3.30	Rat	0.012		0.65	10.0	RLMic	7.14	0.72, 1.30, 16, 15, 11, 0.050, 0.001 in aqueous buffer at pH 1.2, 2.6, 3.1, 3.5, 4.6, 5.7, and 8.0, respectively
					Human	0.049	0.32	0.70	31.5	HLMic		
JNJ8	Ritanserin	478	B 8.20 B 2.07	5.20	Rat	0.015		0.74	139	RLMic	12.0[d]	1.4, 0.063, 0.037in aqueous buffer at pH 2.2, 4.1, and 6.1, respectively
					Human	0.008	0.45	0.65	4.91	HLMic		
JNJ9	Sabeluzole	415	B 7.60 B 3.40	4.63	Rat	0.016		0.84	43.0	RLMic	2.93	13, 5.8, 1.3, 3.9, 0.19, 0.01 in aqueous buffer at pH 2.7, 3.3, 4.2, 4.6, 6.0, and 6.9, respectively
					Human	0.014	0.06	0.82	5.10	HLMic		
JNJ10		297	B 9.47	4.03	Rat	0.141		2.0	312	RLMic	0.321	29, 11, 4.7, 2.9, 0.14, 0.061 in aqueous buffer at pH 3.4, 3.5, 4.5, 7.5, 9.14, and 12.8, respectively
					Human	0.115	0.12[e]	1.4	10.5	HLMic		
JNJ11	Lubeluzole	433	B 7.60 B 4.27	4.88	Rat	0.008		0.76	52.0	RLMic	2.79	0.013 in aqueous buffer at pH 6.9
					Human	0.003	0.05[e]	0.58	3.90	HLMic		
JNJ12		296	B 9.88 B 3.00	1.18	Rat	0.820		1.5	20.8	RLMic	0.05	20, 20, 20, 7.56, 3.09 in aqueous buffer at pH 1.8, 3.8, 4.3, 7.45, and 12.6, respectively
					Human	0.867	0.85[e]	1.5	0.570	HLMic		
JNJ13	Ridogrel	366	A 4.90 B 3.84	3.54	Rat	0.049		0.80	5.10	RLHep	4.73	0.26, 0.02, 0.65, 9.8 in aqueous buffer at pH 2.1, 5.4, 7.0, and 8.1, respectively
					Human	0.033	1.0[f]	0.77	2.20	HLHep		
JNJ14	Laniquidar	584	B 7.90 B 3.30	5.50	Rat	0.002		0.79	51.7	RLMic	4.56[d]	12.4, 0.58, 0.10, 0.064 in aqueous buffer at pH 2.21, 2.78, 3.62, and 7.05, respectively
					Human	0.001	0.08	0.62	99.0	HLMic		
JNJ15	Mazapertine	421	B 7.06	3.96	Rat	0.030		0.63	623	RLMic	5.70[d]	80, 43, 0.54, 0.21, 0.22 in aqueous buffer at pH 3.8, 4.7, 6.9, 8.9, and 11.5, respectively
					Human	0.011	0.13[e]	0.52	231	HLMic		
JNJ16		686	B 7.20 B 3.10	4.12	Rat	0.036		0.78	28.2	RLMic	1.85	13, 1.1, 0.75, 0.04, 0.01 in aqueous buffer at pH 2.2, 3.7, 5.7, 7.5, and 8.6, respectively
					Human	0.034	0.08	0.75	20.3	HLMic		
JNJ17		558	B 7.26 B 6.18 B 4.00 A 8.28	3.90	Rat	0.028		1.0	416	RLMic		
					Human	0.009	0.14[e]	1.0	231	HLMic		
JNJ18	Risperidone	411	B 8.24 B 3.11	3.04	Rat	0.118		0.85	250	RLMic	5.70	40, 4.1, 1.8, 0.25, 0.064 in aqueous buffer at pH 5.4, 6.0, 6.2, 7.5, and 8.7, respectively
					Human	0.100	0.34	0.67	7.96	HLMic		
JNJ19	Levocabastine	420	B 9.90 A 3.20	1.75	Rat	0.465		1.1	1.25	RLHep	2.10	0.06, 0.05, 0.02, 0.02 in aqueous buffer at pH 2.0, 3.2, 6.0, and 8.0, respectively
					Human	0.453	1.0[f]	1.2	0.33	HLHep		
JNJ20	Norcisapride	313	B 9.10 B 3.00	1.51	Rat	0.650		1.5	2.43	RLMic	1.16	80, 92, 93, 74, 41 in aqueous buffer at pH 2.1, 4.8, 6.6, 7.8, and 8.0, respectively
					Human	0.625	0.79[e]	1.6	0.88	HLMic		

TABLE I—*Continued*

JNJ No.	Generic Name	mol. wt.	pK_a	Log P_{ow}	Species	fu_p	fu_{inc} [a]	R_B	In Vivo CL_{int} [b]	Test System	P_{eff} [c,d]	Solubility
									ml/min/kg		10^{-4} *cm/s*	*mg/ml*
JNJ21		481	B 7.27	3.55	Rat	0.015		1.5	35.6	RLMic	1.96	0.05 in aqueous buffer at pH 1.2, 0.003 in SIF at pH 7.53
					Human	0.012	0.23	1.5	77.0	HLMic		
JNJ22		570	A 8.21	4.78	Rat	0.001		0.74	156	RLMic	0.751	0.002 and 100 in aqueous buffer at pH 6.5 and 8.7, respectively and 0.249 in SIF at pH 7.5
					Human	0.001	0.90	0.55	116	HLMic		
JNJ23		359	B 7.00 B 3.10	3.40	Rat	0.082		0.80	208	RLMic	3.41	10.3, 3.9, 0.42, 0.035, 0.002 in aqueous buffer at pH 3.0, 4.2, 5.1, 6.0, and 8.1, respectively
					Human	0.016	0.06	0.61	10.2	HLMic		
JNJ24		380	B 7.23 B 5.20	5.24	Rat	0.007		0.75	371	RLHep	2.00	20, 10.2, 2.19, 0.026 in aqueous buffer at pH 1.4, 4.4, 5.2, and 6.0, respectively and 0.005 SIF at pH 7.4
					Human	0.006	1.0[f]	0.59	8.97	HLHep		
JNJ25		660	B 6.80 B 2.86	4.84	Rat	0.015		0.70	19.9	RLMic	4.54[d]	1.6, 2.43, 0.52, 0.02, 0.01 in aqueous buffer at pH 2.1, 4.4, 5.0, 7.0, and 9.0, respectively
					Human	0.016	0.05[e]	0.72	7.28	HLMic		
JNJ26		500	B 5.95 B 3.67	4.00	Rat	0.036		1.3	24.8	RLHep	2.07	2.3, 0.18, 0.014, 0.005 in aqueous buffer at pH 2.3, 4.5, 5.9, and 7.5
					Human	0.023	1.0[f]	1.5	9.03	HLHep		

A, acid; B, base; HLHep, human liver hepatocytes; HLMic, human liver microsomes; log RLHep, rat liver hepatocytes; RLMic, rat liver microsomes.
[a] Experimental values of fu_{inc} in human microsomal protein were determined according to the method of Giuliano et al. (2005). Rat fu_{inc} was assumed to equal human fu_{inc}.
[b] In vivo CL_{int} was calculated using eq. 6 as described under *Materials and Methods*.
[c] Permeability was measured using a Caco-2 assay and converted to P_{eff} using the reported correlation $\log P_{eff,human} = 0.6532 \cdot \log P_{app,caco-2} - 0.3036$ (Sun et al., 2002).
[d] In silico predicted P_{eff} (ADMETPredictor software version 1.30.2; Simulations Plus Inc.).
[e] Predicted fu_{inc} value in microsomes was determined according to the method of Austin et al. (2002).
[f] Hepatocyte incubation was performed in protein-free medium ($fu_{inc} = 1$).

marrow, and rest of the body, which were linked by the venous and arterial blood circulation. It was assumed that drug distributes instantaneously and homogenously within each tissue compartment, and uptake of drug within each tissue compartment was limited by the blood flow (perfusion rate-limited uptake). The default Gastroplus settings of all physiological data used in the rat and human PBPK models are summarized in Table 3. The methods used for estimating the PBPK model input data on CL_H, renal plasma clearance (CL_R), P_{tp} values, and absorption rate are described below.

Prediction of Human and Rat P_{tp} and V_{ss}: Method Vd1. Predicted values of rat and human P_{tp} for each tissue compartment of Fig. 1 were obtained from drug-specific physicochemical parameters using the following mechanistic tissue composition-based equation developed by Poulin and coworkers (Poulin and Theil, 2002):

$$P_{tp} = \frac{[P \cdot (V_{NLT} + 0.3 \cdot V_{PHT}) + (V_{WT} + 0.7 \cdot V_{PHT})] \cdot fu_p}{[P \cdot (V_{NLp} + 0.3 \cdot V_{PHp}) + (V_{Wp} + 0.7 \cdot V_{PHp})] \cdot fu_t} \quad (1)$$

where P is the anti-logged value of log P_{ow} for a nonadipose tissue or is the vegetable oil/buffer partition coefficient for both the ionized and nonionized species at pH 7.4 (D_{vow}) for adipose tissue. D_{vow} was calculated from log P_{ow} using the Henderson-Hasselbalch equations and the following relationship: log $P_{vow} = 1.115 \cdot \log P_{ow} - 1.35$ (Leo et al., 1971). V is the fractional tissue volume content of neutral lipids (NL), phospholipids (PH), or water (W) in tissue (T) and plasma (p). The physiological data on human and rat values used for V_{NLT}, V_{NLp}, V_{PHT}, V_{PHp}, V_{WT}, and V_{Wp} have been described in the literature (Poulin and Theil, 2002). The fraction unbound in tissue (fu_t) in eq. 1 was estimated as follows:

$$fu_t = 1/(1 + (((1 - fu_p)/fu_p) \cdot RA)) \quad (2)$$

where RA is the ratio of albumin concentration found in tissue over plasma. For lipophilic and highly protein-bound compounds, it has been assumed that for adipose tissue, RA equals 0.15, whereas for nonadipose tissue, RA equal 0.5 (Ellmerer et al., 2000; Poulin and Theil, 2002).

Finally, rat and human V_{ss} values were calculated by Gastroplus software according to the equation of Sawada et al. (1984) in which V_{ss} equals the plasma volume in addition to the sum of each P_{tp} multiplied by its respective tissue volume.

Prediction of Human and Rat P_{tp} and V_{ss}: Method Vd2. For rat P_{tp} and V_{ss}, experimental rat P_{tp} values were determined under in vivo conditions (single oral or intravenous dose) as the ratio of the AUC calculated over a minimum of five time points, assuming pseudoequilibrium. All experimentally determined in vivo rat P_{tp} values used within this study are summarized in Table 2. In instances where the in vivo P_{tp} was not available for a compound, the value for that tissue compartment (Fig. 1) was predicted using the tissue composition-based equation as described by Rodgers et al. (2005a). In brief, for strong bases (p$K_a > 7.0$), P_{tp} of unbound drug (P_{tpu}) was calculated using eq. 3:

$$P_{tpu} = \frac{P_{tp}}{fu_p} = \left[V_{EW} + \frac{1 + 10^{pKa\text{-}7.0}}{1 + 10^{pKa\text{-}7.4}} \cdot V_{IW} + \frac{K_a \cdot [AP]_t \cdot 10^{pKa\text{-}7.0}}{1 + 10^{pKa\text{-}7.4}} + \frac{P_{vow} \cdot V_{NL} + ((0.3 \cdot P_{vow} + 0.7) \cdot V_{NP})}{1 + 10^{pKa\text{-}7.4}} \right] \quad (3)$$

where V is the fractional tissue volume of neutral lipids (NL), neutral phospholipids (NP), extracellular water (EW), and intracellular water (IW), $[AP]_t$ is the concentration of acidic phospholipids in tissue, all physiological data on V_{EW}, V_{IW}, V_{NL}, V_{NP} and $[AP]_t$ for both adipose and nonadipose tissue have been described in the literature (Rodgers et al., 2005a), pK_a represents the dissociation constant of the protonated base, and P_{vow} is the anti-logged value of log P_{vow} (calculated from P_{ow} as described above). K_a is the association constant of the compound with the acidic phospholipids, and was calculated from eq. 4:

TABLE 2

Summary of the preclinical (rat) and clinical pharmacokinetic data for the 26 compounds

JNJ No.	Species	Dose	Route	CL or CL/*F*	CL_R	V_{ss} or V_d/F	In Vivo $t_{1/2}$	C_{max}	AUC	Experimentally Determined In Vivo Rat P_{tp}[a]										
										Lung	Adipose	Muscle	Liver	Spleen	Heart	Brain	Kidney	Skin	Testes	Bone
		mg		*l/h*		*liters*	*h*	*ng/ml*	*ng · h/ml*											
JNJ1	Human	100	i.v.	71.6		413	5.10		1.40E + 03											
	Human	100	p.o.	202		1.49E + 03		60.1	494											
	Rat	2.50	i.v.	1.55		3.92	2.91		1.61E + 03	19.4	5.27	6.50	0.571	10.3	2.91	1.52	5.68			
	Rat	1.88	p.o.	4.24					442											
JNJ2	Human	10.0	i.v.	34.3		157	7.59		292											
	Human	60.0	p.o.	232		2.54E + 03		102	259											
	Rat	0.625	i.v.	1.30		1.39	0.871		480	10.9	3.21	3.45	13.8		3.87		22.5	4.35		
	Rat	0.625	p.o.	6.01					104											
JNJ3	Human	0.500	i.v.	80.5		1.14E + 03	10.40		6.20											
	Human	5.00	p.o.	192		2.87E + 03		2.01	26.1											
	Rat	0.313	i.v.	0.736		1.55	1.37		425	99.7	2.67	2.95	14.1	15.6	4.71	3.73	10.6	7.65	5.32	7.87;14.1
	Rat	0.313	p.o.	0.925					338											
JNJ4	Human	8.00	i.v.	17.8	3.93	175	7.40		482											
	Human	8.00	p.o.	18.7		200		42.6	427											
	Rat	0.625	i.v.	0.473	0.100	1.30	3.48		1.32E + 03	4.42	0.476	2.14	2.53	2.92	2.28	1.51	14.5	1.14	1.46	4.79;4.81
	Rat	0.625	p.o.	0.803					778											
JNJ5	Human	8.75	i.v.	21.2		28.8	1.37		510											
	Human		p.o.																	
	Rat	4.00E02	i.v.	0.464		0.110	0.146		86.2	1.11	3.01	0.440	1.43	1.05	0.791	0.181	1.18	0.512	0.481	
	Rat		p.o.																	
JNJ6	Human	0.350	i.v.	49.6		128	2.47		8.10											
	Human		p.o.																	
	Rat	6.25E04	i.v.	1.04		0.967	1.05		0.604	6.18	7.72	1.71	0.370	2.80	1.80	2.08	1.17		1.97	
	Rat		p.o.																	
JNJ7	Human	10.0	i.v.	33.9		268	14.3		298											
	Human	20.0	p.o.	71.7		1.48E + 03		71.4	279											
	Rat	2.50	i.v.	5.75E-02		0.168	2.00		4.35E + 04	1.49	0.562	0.284	2.60	0.911	0.354	0.194	1.53	0.463	0.495	0.19;0.18
	Rat	2.50	p.o.	9.82E02					2.55E + 04											
JNJ8	Human	5.00	i.v.	2.14		99.0	40.0		2.51E + 03											
	Human	10.0	p.o.	2.33		134		164	4.30E + 03											
	Rat	0.625	i.v.	0.400		2.00	2.52		1.56E + 03	27.8	4.29	3.02	21.8			10.5	14.1			
	Rat	0.625	p.o.	0.918					681											
JNJ9	Human	10.0	i.v.	17.0		385	18.9		594											
	Human	5.00	p.o.	22.7		621		14.5	220											
	Rat	0.313	i.v.	0.538		1.46	2.13		581	29.2	8.41	0.831	37.7	5.48	2.45	5.37	10.4	2.95	4.62	1.83;7.76
	Rat	0.625	p.o.	1.24					506											
JNJ10	Human	1.00	i.v.	149		1.33E + 03	7.09		6.58											
	Human	8.00	p.o.	950		9.72E + 03		0.590	8.42											
	Rat	2.50	i.v.	2.02		8.37	2.77		1.24E + 03	400		20.1	150		40.2	80.3	80.1		75.1	
	Rat	10.0	p.o.	5.26					1.90E + 03											

TABLE 2—*Continued*

JNJ No.	Species	Dose	Route	CL or CL/*F*	CL_R	V_{ss} or V_d/F	In Vivo $t_{1/2}$	C_{max}	AUC	Experimentally Determined In Vivo Rat P_{tp}[a]										
										Lung	Adipose	Muscle	Liver	Spleen	Heart	Brain	Kidney	Skin	Testes	Bone
		mg			*l/h*	*liters*	*h*	*ng/ml*	*ng · h/ml*											
JNJ11	Human	10.0	i.v.	8.46		181	17.6		1.22E + 03											
	Human	10.0	p.o.	13.1		333		52.6	763											
	Rat	0.158	i.v.	0.375		1.06	2.05		420	18.1	13.8	2.04	31.7	7.51	3.66	4.13	9.91	4.62	6.32	2.67;11.1
	Rat		p.o.																	
JNJ12	Human	30.0	i.v.	16.6	9.24	122	8.20		196											
	Human	30.0	p.o.	184		2.18E + 03		15.6	163											
	Rat	1.25	i.v.	0.550	0.300	1.77	2.90		2.27E + 03	7.17		1.01	45.9		2.81	1.02	10.7	1.03		
	Rat	0.625	p.o.	78.1					8.00											
JNJ13	Human	100	i.v.	4.41		30.3	7.54		2.29E + 03											
	Human	400	p.o.	4.61		50.2		1.71E + 04	8.67E + 04											
	Rat	2.50	i.v.	3.00E-02		0.194	5.10		8.33E + 04	0.371		0.111	1.39		0.389	0.178	0.251			
	Rat	2.50	p.o.	4.07E-02					6.15E + 04											
JNJ14	Human	50.0	i.v.	59.4		422	10.6		882											
	Human	200	p.o.	568		8.69E + 03		187	352											
JNJ15	Human	2.80	i.v.	25.9		108	4.60													
	Human	40.0	p.o.	56.4		374			0.650											
	Rat	1.25	i.v.	0.588		0.433	1.94		2.13E + 03	2.31	8.01	1.49	20.5	1.55	1.52	0.620	7.36	1.12	0.762	
	Rat	7.50	p.o.	2.96					2.54E + 03											
JNJ16	Human	50.0	i.v.	36.0		717	18.9		1.37E + 03											
	Human	200	p.o.	68.1		1.86E + 03		220	2.94E + 03											
	Rat	0.500	i.v.	0.370		1.46	2.92		1.35E + 03	46.7		3.24	35.5	20.9	7.73	0.661	14.1		2.35	
JNJ17	Human	75.0	i.v.	31.2		172	5.14		2.45E + 03											
	Human		p.o.																	
	Rat	0.500	i.v.	1.40		15.4	6.67		357	56.1	15.3	20.5	48.2	50.4	40.1	1.12	92.3	10.1	2.11	
	Rat	2.50	p.o.																	
JNJ18	Human	1.00	i.v.	23.6	0.780	81.0	2.80		45.3											
	Human	1.00	p.o.	31.3		126		7.90	32.0											
	Rat	0.313	i.v.	0.962		0.443	0.600		325	3.42		0.581	12.3		0.822	0.233	6.43			
	Rat	0.313	p.o.	3.52					88.8											
JNJ19	Human	0.200	i.v.	1.82	1.26	82.2	33.0		115											
	Human	2.00	p.o.	1.75		83.4		23.0	1.14E + 03											
	Rat	2.50E02	i.v.	4.05E02	0.013	0.340	6.00		617	1.49	0.840	0.883	14.0	1.32	1.19	0.589	8.52	0.978	0.982	0.52;1.56
	Rat	0.625	p.o.	4.87E02					1.28E + 04											
JNJ20	Human		i.v.		25.2															
	Human	15.0	p.o.	56.4		646	9.00	36.1	266											
	Rat	1.25	i.v.	0.605	0.350	1.59	2.30		2.07E + 03											
	Rat	2.50	p.o.	1.11					2.24E + 03											

TABLE 2—*Continued*

JNJ No.	Species	Dose	Route	CL or CL/*F*	CL_R	V_{ss} or V_d/F	In Vivo $t_{1/2}$	C_{max}	AUC	Experimentally Determined In Vivo Rat P_{tp}[a]										
										Lung	Adipose	Muscle	Liver	Spleen	Heart	Brain	Kidney	Skin	Testes	Bone
		mg		*l/h*		*liters*	*h*	*ng/ml*	*ng · h/ml*											
JNJ21	Human		i.v.																	
	Human	150	p.o.	773		3.04E + 03	21.2	39.3	194											
	Rat	0.250	i.v.	0.410		2.68	5.86		610			7.25	23.3		6.91	4.35				
	Rat	1.25	p.o.	1.10					1.14E + 03											
JNJ22	Human		i.v.																	
	Human	300	p.o.	602		687	1.40	301	498											
	Rat	6.25	i.v.	0.175		5.25E-02	1.20		3.57E + 04											
	Rat	10.0	p.o.	0.730					1.37E + 04											
JNJ23	Human		i.v.																	
	Human	16.0	p.o.	17.9		53.4	3.50	314	894											
	Rat	0.375	i.v.	0.500		0.369	0.545		750	2.48	2.53	0.665	8.64	3.35	1.34	1.39	4.03	0.915	1.72	0.69;3.79
	Rat	1.33	p.o.	1.65					803											
JNJ24	Human		i.v.																	
	Human	80.0	p.o.	26.5		635	26.6	551	3.02E + 03											
	Rat	0.625	i.v.	0.829		0.947	2.40		754	3.43	3.36	4.36	27.9	2.53	2.65	1.00	4.89	0.936	4.53	0.58;2.54
	Rat	1.25	p.o.	9.77					128											
JNJ25	Human		i.v.																	
	Human	200	p.o.	19.9		413	22.7	701	1.01E + 04											
	Rat	0.625	i.v.	0.320		1.735	4.33		1.95E + 03	20.6	3.80	2.27	11.7	6.74	4.27	0.663	2.96	1.09	0.666	0.63;2.44
	Rat	1.25	p.o.	0.373					3.35E + 03											
JNJ26	Human		i.v.																	
	Human	20.0	p.o.	38.8		292	9.80	99	516											
	Rat	0.625	i.v.	0.365		0.609	1.47		1.71E + 03	2.51	20.0	1.20	2.10	1.10	1.70	0.500	2.00	2.51	2.11	2.72;20.0
	Rat	2.50	p.o.	11.1					226											

[a] Experimental rat P_{tp} values were determined under in vivo conditions (single oral or intravenous dose) as the ratio of the AUC calculated over a minimum of five time points, assuming pseudoequilibrium. Underlined values refer to in vivo rat P_{tp} obtained using total radioactivity measurements.

TABLE 3

Physiological values for tissue volumes and blood flow in rat and human

Default values taken from Gastroplus software 5.10.0 generic rat and human PBPK model.

Tissue	Rat		Human	
	Blood Flow	Volume	Blood Flow	Volume
	ml/min	*ml*	*l/min*	*liters*
Lung	53.0	2.10	6.08	1.11
Spleen	0.600	0.600	0.184	0.184
Liver	13.8	10.3	1.50	1.63
ACAT gut	7.50		0.836	
Adipose	0.400	10.0	0.605	30.3
Muscle	7.50	122	0.622	20.7
Heart	3.90	1.20	0.230	0.315
Brain	1.30	1.24	0.882	1.73
Kidney	9.20	3.70	1.02	0.277
Skin	5.80	40.0	0.235	1.96
Testes	0.500	2.50	0.007	0.032
Red marrow	1.30	1.33	0.354	1.18
Yellow marrow	0.275	2.81	0.098	3.28
Rest of body	9.01	41.5	0.529	17.6
Arterial blood	53.0	5.60	6.08	2.21
Venous blood	53.0	11.3	6.08	4.42

$$K_{a,BC} = \left[P_{tpu,BC} - \frac{1 + 10^{pKa-7.22}}{1 + 10^{pKa-7.4}} \cdot V_{IW} - \frac{P_{vow} \cdot V_{NL,BC} + (0.3 \cdot P_{vow} + 0.7) \cdot V_{NP,BC}}{1 + 10^{pKa-7.4}} \right] \cdot \left[\frac{1 + 10^{pKa-7.4}}{[AP]_{BC} \cdot 10^{pKa-7.22}} \right] \quad (4)$$

where $P_{tpu,BC}$ is the P_{tpu} of the red blood cell (BC) and thus equals the erythrocyte-to-plasma concentration ratio (E/P) divided by fu_p. E/P was calculated from the R_B and hematocrit (H), as follows: $E/P = (R_B - (1 - H))/H$. For weak bases ($pK_a < 7$; JNJ5, JNJ25, JNJ26), acids (JNJ13, JNJ22), and zwitterions (JNJ17, JNJ19) P_{tp} values were predicted using a modification of eq. 3, as described by Rodgers and Rowland (2006). It should be noted that for all compounds, P_{tp} estimates for testes and rest of body compartment were taken from method Vd1, since the published equations by Rodgers and Rowland (2006) do not allow for prediction of these values.

For human P_{tp} and V_{ss}, all rat P_{tp} values obtained as described in this section were scaled to human with the assumption that the human P_{tpu} is equal to the rat P_{tpu}:

$$\text{Human } P_{tp} = \frac{\text{Human } fu_p \cdot \text{Rat } P_{tp}}{\text{Rat } fu_p} \quad (5)$$

Finally, rat and human V_{ss} values were calculated by Gastroplus software (Simulations Plus Inc.) as mentioned under method Vd1.

Prediction of CL_H, CL_R, and CL: Method CL1. For metabolically cleared compounds, the liver compartment of the PBPK model was provided with input data on CL_H, which was calculated in three steps.

First, the in vitro hepatic CL_{int} (l/h/mg microsomal protein or l/h/10^6 cells) was determined from a typical microsomal or hepatocyte substrate depletion or kinetic assay (Kantharaj et al., 2003), and was scaled to in vivo CL_{int} (l/h), accounting for the microsomal recovery or hepatocellularity and liver weight as described by Houston (1994):

$$\text{in vivo } CL_{int} = \text{in vitro } CL_{int} \cdot SF \quad (6)$$

where SF (scaling factor) represents the milligrams of microsomal protein or million cells per gram of liver multiplied by the grams of liver weight. A microsomal recovery of 40 mg of microsomal protein/g of liver (Pelkonen et al., 1973; Ito and Houston, 2005) was used for both rat and human. A hepatocellularity of 125 and 120 million cells/g of liver was used for rat and human, respectively (Iwatsubo et al., 1996, 1997). Human and rat standard liver weight was 1400 g (20 g/kg body weight) and 11.25 g (45 g/kg body weight), respectively (Houston, 1994; Obach et al., 1997).

Second, the hepatic blood clearance ($CL_{H,blood}$,) was calculated using the commonly used equation of the well stirred liver model:

$$CL_{H,blood} = \frac{(fu_p/R_B) \cdot Q_h \cdot (\text{in vivo } CL_{int}/fu_{inc})}{Q_h + (\text{in vivo } CL_{int}/fu_{inc}) \cdot (fu_p/R_B)} \quad (7)$$

where Q_h is the hepatic blood flow (human, 90 l/h; rat, 0.828 l/h). Experimental values for fu_p, fu_{inc}, R_B, and in vivo CL_{int} are presented in Table 1. Third, because Gastroplus requires input data on CL_H, $CL_{H,blood}$ was converted to CL_H ($CL_H = R_B \cdot CL_{H,blood}$).

For renally cleared compounds, the prediction of human CL_R was obtained using the glomerular filtration rate (GFR) ratio approach as described by Lin (1998):

$$\text{Human } CL_{R,unbound} = \frac{\text{Rat } CL_{R,unbound}}{\text{GFR ratio}} \quad (8)$$

where rat $CL_{R,unbound}$ (l/h/kg) is the CL_R corrected for rat fu_p (CL_R/fu_p) and the GFR ratio between rat and human is 4.8 (Lin, 1998). Predicted CL was calculated as the sum of the predicted CL_H and CL_R.

Prediction of CL_H, CL_R, and CL: Method CL2. Our previous study and those by others using in vitro metabolism data have suggested that in vitro CL_{int} may provide a better estimate of in vivo CL_H of total rather than unbound drug (Obach et al., 1997; De Buck et al., 2007). Therefore, CL_H predictions were also assessed using method CL2 under the assumption that fu_p/R_B and fu_{inc} effectively nullify in the liver model calculation, negating the measurement of either process:

$$CL_{H,blood} = \frac{Q_h \cdot \text{in vivo } CL_{int}}{Q_h + \text{in vivo } CL_{int}} \quad (9)$$

$CL_{H,blood}$ was converted to CL_H as described above. The prediction of human CL_R from rat data was identical to that found by method CL1. Predicted CL was calculated as the sum of the predicted CL_H and CL_R.

Prediction of in Vivo $t_{1/2}$: Method Vd1/CL1 and Method Vd2/CL2. Prediction of in vivo $t_{1/2}$ relies on the prediction of both V_{ss} and CL. Two different approaches were tested for their ability to predict in vivo $t_{1/2}$. First, method Vd1 was combined with method CL1 (i.e., method Vd1/CL1) since this combination predicts CL_H according to the most widely accepted approach toward the use of fu_p/R_B and fu_{inc} (eq. 7) (Jones et al., 2006a), and requires minimal data input for prediction of V_{ss}. For comparison, method Vd2 was combined with method CL2 (i.e., method Vd2/CL2) since this combination predicts V_{ss} and CL according to this approach, which was also found to provide the best results in rat. Predicted values of in vivo $t_{1/2}$ were taken from the Gastroplus software interface (Simulations Plus Inc.).

The ACAT Model and Prediction of Oral AUC. Prediction of oral AUC relies on the prediction of both CL and the extent of absorption. CL was predicted using either method CL1 or method CL2 as described above. The extent of absorption was predicted using the Gastroplus ACAT model (Yu and Amidon, 1999; Agoram et al., 2001). For all simulations, the ACAT model was provided with experimentally determined data on log P_{ow}, pK_a, aqueous buffer solubility or solubility in SIF at defined pH, effective human jejunal permeability (P_{eff}), and dose (D) administered (Table 1). Apparent permeability (P_{app}) was measured using a typical Caco-2 permeability assay and converted to P_{eff} using the following correlation: $\log P_{eff,human} = 0.6532 \cdot \log P_{app,caco-2} - 0.3036$ (Sun et al., 2002). In instances where Caco-2 data were not available ($n = 4$, Table 1), in silico estimates of human P_{eff} were obtained by the artificial neural network model in ADMETPredictor version 1.3.2 (Simulations Plus Inc.). The extent to which paracellular and transcellular routes are used in drug transport is influenced by the fraction of ionized and un-ionized species, which, in turn, depends upon the pK_a of the drug and the pH of the solution (Ungell et al., 1998). To account for such regional changes in permeability, the Gastroplus built-in "Opt logD-model" was applied (for a detailed description, see manual of Gastroplus 5.1.0). In brief, the model assumes that the regional absorption rate coefficient for each gastrointestinal compartment can be calculated as the product of the P_{eff} (jejunal permeability at pH 6.5) and an absorption scale factor (ASF) specific for each gastrointestinal compartment. An estimate of ASF for each compartment is obtained based on the premise that a linear relationship with a negative slope exists between the deviation of

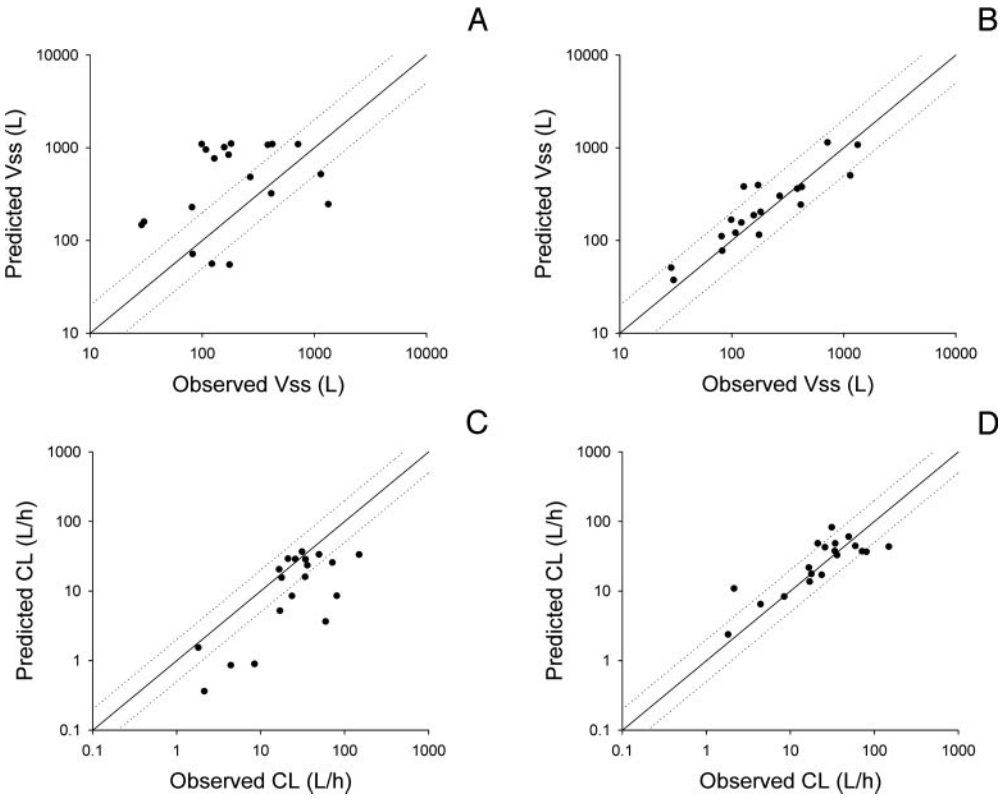

FIG. 2. A and B, prediction accuracy for the physiologically based predictions of human V_{ss} obtained using method Vd1 (A) and method Vd2 (B). C and D, prediction accuracy for the physiologically based predictions of human total body clearance from plasma (CL) obtained using method CL1 (C) and method CL2 (D). For more details on all methods used, refer to *Materials and Methods*. Lines signify unity and 2-fold errors between predicted and experimentally determined parameters.

TABLE 4

Statistics for the predicted human pharmacokinetic parameters obtained using method Vd1 and method CL1

See *Materials and Methods* for more details on prediction of each parameter using method Vd1 and/or method CL1.

Parameter	*n*	*afe*	*rmse*	Percentage within 2-fold Error	Percentage within 3-fold Error
Vss (l)	19	2.10	604	31.6	52.6
CL (l/h)	19	2.41	36.3	52.6	68.4
CL_R (l/h)	4	1.09	5.41	100	100
In vivo $t_{1/2}$ (h)	26	5.40	903	26.9	38.5
V_d/F (liters)	23	1.38	9.33E + 03	21.7	39.1
AUC (ng · h/ml)	23	5.09	7.91E + 04	34.8	43.5
C_{max} (ng/ml)	23	1.39	2.94E + 03	65.2	69.6
F (%)	16	1.60	31.0	62.5[a]	

[a] Percentage within 1.5-fold error.

the log D from the neutral log P ($\Delta\log D_{pH}$) and the change in the log of the permeability coefficients at the two pH values:

$$ASF_{pH} = C2 \cdot 10^{C1 \cdot \left(\frac{\Delta\log D_{pH}-6.26}{\Delta\log D_{6.5}-6.26}\right)} \quad (10)$$

where C1 and C2 are two proprietary fitted constants accomplished through a series of many thousands of simulations. The Gastroplus ACAT physiology was "Human-Physiological-Fasted". Metabolic first-pass extraction was assumed to depend only on CL_H.

Prediction of V_d/F and C_{max} after Oral Dosing. Prediction of both V_d/F and C_{max} rely on the prediction of V_{ss}, CL, and the rate and extent of absorption. The rate and extent of absorption were predicted using the ACAT model as described above. V_{ss} and CL were predicted using either method Vd1/CL1 or method Vd2/CL2 as described above. Predicted values of C_{max} were taken from the Gastroplus software interface (Simulations Plus Inc.). The predicted V_d/F was calculated from the predicted CL/F multiplied by the predicted in vivo $t_{1/2}$/ln 2. Predicted CL/F was calculated as D divided by predicted AUC after oral dosing.

Prediction of Plasma Concentrations after Oral Dosing. Predictions of individual plasma concentrations after oral dosing were obtained using the ACAT model (as described above), which served as a time-dependent input to the disposition model composed of either method Vd1/CL1 or method Vd2/CL2 as described above.

Calculation of the in Vivo Pharmacokinetic Parameters. Noncompartmental analysis was performed using WinNonLin version 4.01 (Pharsight, Mountain View, CA) to calculate CL from the relationship CL = D/AUC, and V_{ss} was determined as V_{ss} = Dose · AUMC/(AUC)^2. Absolute oral bioavailability (F) was calculated as the ratio of dose-normalized AUC after oral and intravenous administration using the mean of individual AUCs.

Success Criteria. Success of predictions was assessed by the root mean squared prediction error (*rmse*) and the average-fold error (*afe*) as measures of precision and bias, respectively, with equal value to under- and overpredictions:

$$mse = \frac{1}{N}\sum(\text{Predicted} - \text{Observed})^2, \; rmse = \sqrt{mse} \quad (11)$$

$$afe = 10^{\left|\frac{\sum \log \frac{\text{Predicted}}{\text{Observed}}}{N}\right|} \quad (12)$$

TABLE 5

Statistics for the predicted human pharmacokinetic parameters obtained using method Vd2 and method CL2

See *Materials and Methods* for more details on prediction of each parameter using method Vd2 and/or method CL2.

Parameter	*n*	*afe*	*rmse*	Percentage within 2-fold Error	Percentage within 3-fold Error
V_{ss} (liters)	19	1.14	207	84.2	94.7
CL (l/h)	19	1.10	31.3	73.7	89.5
CL_R (l/h)	4	1.09	5.41	100	100
In vivo $t_{1/2}$ (h)	26	1.49	8.72	69.2	88.5
V_d/F (liters)	23	1.32	2.10E + 03	69.6	82.6
AUC (ng · h/ml)	23	1.06	6.45E + 03	73.9	87.0
C_{max} (ng/ml)	23	1.31	2.01E + 03	65.2	91.3
F (%)	16	1.06	15.0	81.3[a]	

[a] Percentage within 1.5-fold error

TABLE 6

Effect of plasma protein binding and source of rat P_{tp} data on prediction accuracy of human V_{ss} using method Vd2

For more details on method Vd2, see *Materials and Methods*.

Parameter	*n*	fu_p Correction[a]	Source of Rat P_{tp} Data	*afe*	*rmse*	Percentage within 2-fold Error	Percentage within 3-fold Error
V_{ss} (liters)	19	Yes	Predicted + Experimental[b]	1.14	207	84.2	94.7
V_{ss} (liters)	19	No	Predicted + Experimental[b]	1.54	361	52.6	68.4
V_{ss} (liters)	19	Yes	Predicted[c]	1.44	377	47.4	78.9
V_{ss} (liters)	19	No	Predicted[c]	1.89	600	42.1	78.9

[a] "Yes" refers to the assumption that human unbound P_{tp} is equal to rat unbound P_{tp}; "No" refers to the assumption that human P_{tp} is equal to rat P_{tp}.
[b] In instances where the experimental in vivo rat P_{tp} was not available, the value for that particular tissue was predicted as described for method Vd2. All experimentally determined in vivo rat P_{tp} values are given in Table 2.
[c] Only predicted rat P_{tp} values were used for all tissue compartments. All values were predicted as described for method Vd2.

TABLE 7

Statistics for the predicted rat pharmacokinetic parameters

For more details on methods Vd1, Vd2, CL1, and CL2, see *Materials and Methods*.

Parameter	Method	Source of Rat P_{tp} Data	*afe*	*rmse*	Percentage within 2-fold Error	Percentage within 3-fold Error
V_{ss} (liters)	Vd1	Predicted[a]	1.07	3.23	42.3	53.8
V_{ss} (liters)	Vd2	Predicted + Experimental[b]	1.51	2.52	73.1	88.5
V_{ss} (liters)	Vd2	Predicted[a]	1.10	3.10	65.4	80.8
CL (l/h)	CL1		3.59	0.468	34.6	53.8
CL (l/h)	CL2		1.23	0.311	84.6	100

[a] Only predicted rat P_{tp} values were used for all tissue compartments.
[b] In instances where the experimental in vivo rat P_{tp} was not available, the value for that particular tissue compartment was predicted as described for method Vd2. All experimentally determined in vivo rat P_{tp} values are given in Table 2.

A prediction method with an *afe* ≤ 2 was considered successful. Predicted PK parameters and plasma concentration-time profiles were deemed accurate if they agreed with mean experimental in vivo values within a factor of 2 (Obach, 1999; Poulin and Theil, 2002).

Results

Prediction of V_{ss}. There were 19 compounds that had human intravenous PK data suitable for assessment of V_{ss} predictions. The correlations between observed and predicted human V_{ss} using methods Vd1 and Vd2 are presented in Fig. 2, A and B, respectively. The parameters for the accuracy of the predictions using methods Vd1 and Vd2 are given in Tables 4 and 5, respectively. The simplest approach (method Vd1) predicted human V_{ss} within 2-fold of observed for only 6 compounds (32%, Fig. 2A). In contrast, method Vd2 resulted in more accurate predictions with 16 compounds within 2-fold of observed (84%, Fig. 2B). Although method Vd2 showed slight bias toward overprediction, the bias and precision were typically much better than with method Vd1 as indicated by the decreased *afe* and *rmse* values (Tables 4 and 5). Using method Vd2, the correction for differences in plasma binding between rat and human resulted in better predictions than when binding differences were ignored (Table 6). Ignoring binding differences yielded more bias and a lower precision, but also a decrease in the number of compounds that were within 2-fold error (Table 6). Furthermore, if in Method Vd2 all experimentally determined in vivo rat P_{tp} values were substituted by their predicted counterparts, a general decrease in accuracy was observed, irrespective of correction for plasma binding (Table 6).

V_{ss} prediction accuracy was also assessed in rat to test whether a successful prediction approach in rat indicates that prediction in human would be successful. Method Vd2 was the best predictor of rat V_{ss}, with 73% within 2-fold of observed ($n = 26$) (Table 7). As expected, when all experimentally determined in vivo rat P_{tp} values were substituted by their predicted counterparts, a general decrease in accuracy of method Vd2 was observed. The poorest predictor was method Vd1, which predicted only 12 compounds of 26 within 2-fold of observed (42%, Table 7).

Prediction of CL. The accuracy of clearance predictions refers to the total plasma clearance (CL) when intravenous data were available ($n = 19$). The correlations between observed and predicted human CL using method CL1 are shown in Fig. 2C. Method CL1, which included both blood and microsomal or hepatocyte binding, yielded several

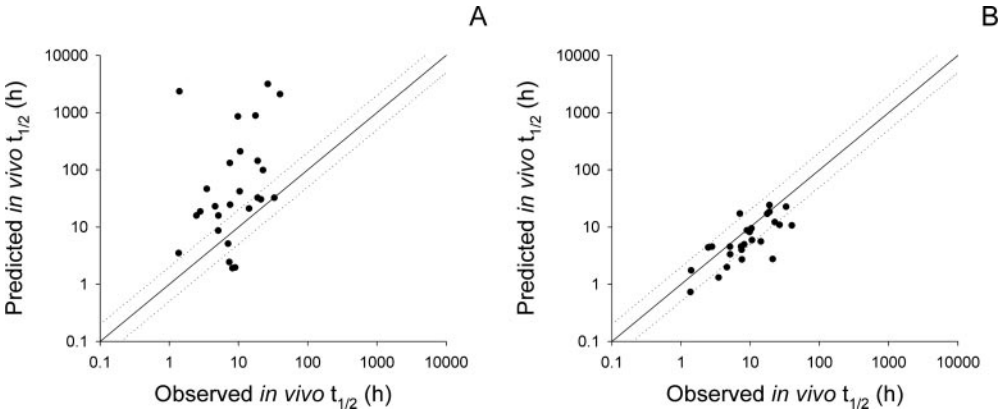

FIG. 3. Prediction accuracy for the physiologically based predictions of human in vivo terminal half-life (in vivo $t_{1/2}$) obtained using method Vd1/CL1 (A) and method Vd2/CL2 (B). For more details on all methods used, refer to *Materials and Methods*. Lines signify unity and 2-fold errors between predicted and experimentally determined parameters.

underpredictions of CL, and only 10 compounds were predicted within 2-fold of mean observed values (53%, Table 4). As a result, a strong bias (*afe*) and poor precision (*rmse*) were observed (Table 4). Despite the overall poor accuracy of the method, prediction of the renal component, i.e., CL_R, was found to be accurate. CL_R predictions ($n = 4$) were 6.4 l/h, 18 l/h, 0.74 l/h, and 19 l/h for JNJ4, JNJ12, JNJ19, and JNJ20, respectively, and therefore, all predictions were within 2-fold of observed (Table 4).

The correlations between observed and predicted human CL using method CL2 are shown in Fig. 2D. This method predicted CL within 2-fold of observed for 14 compounds (74%, Fig. 2D). Predictions showed limited *afe*, and *rmse* value was strongly decreased compared with method CL1 (Table 5). To further substantiate these findings, prediction of CL using both methods CL1 and CL2 was also assessed in rat for all compounds ($n = 26$). Table 7 indicates that method CL2 yielded more accurate predictions in rat compared with method CL1. Method CL1 projected rat CL within a 2-fold error for only 9 compounds (35%), whereas method CL2 projected rat CL within 2-fold error for 22 compounds (85%).

Prediction of in Vivo $t_{1/2}$. The accuracy of the in vivo $t_{1/2}$ predictions refers to the terminal in vivo $t_{1/2}$ after intravenous administration when intravenous data were available ($n = 19$), and to the terminal in vivo $t_{1/2}$ after oral dosing when only oral data were available ($n = 7$). Fig. 3, A and B illustrate the correlations between the observed and predicted values of in vivo $t_{1/2}$ using method Vd1/CL1 and method Vd2/CL2, respectively. Method Vd1/CL1 was a poor predictor of in vivo $t_{1/2}$ in this analysis in that only seven compounds were within 2-fold of observed (27%, Fig. 3A), with high bias toward overprediction (*afe*) and poor precision (*rmse*) (Table 4). These results were expected based on the results of the individual methods Vd1 and CL1. In contrast, method Vd2/CL2 resulted in more accurate predictions of in vivo $t_{1/2}$ with 18 compounds within 2-fold of observed (69%, Fig. 3B). More importantly, there was significantly less bias (*afe*) and higher precision (*rmse*) (Table 5).

Prediction of AUC and *F* after Oral Dosing. There were 23 compounds that had human oral PK data for assessment of oral AUC, and 16 compounds that had both intravenous and oral PK data for assessment of *F*. The correlations between the observed and predicted oral AUC and *F* were obtained using the ACAT model in combination with either method CL1 or method CL2 and are presented in Fig. 4, A and B, respectively. Method CL1 predicted oral AUC within 2-fold of observed for only 8 compounds (35%, Fig. 4A), and a strong bias toward overprediction was observed for both oral AUC (Fig. 4A) and F (Fig. 4A, inset). In contrast, method CL2 predicted oral AUC within 2-fold of observed for 17 compounds (74%, Fig. 4B). Prediction of both oral AUC (Fig. 4B) and *F* (Fig. 4B, inset) showed less bias and higher precision as indicated by a decreased *afe* and *rmse* value (Tables 4 and 5), respectively.

Prediction of V_d/F and C_{max} after Oral Dosing. The accuracy of the V_d/F predictions was assessed on all compounds intended for the oral route ($n = 23$). Figure 5 illustrates the correlations between the observed and predicted values of V_d/F using the ACAT model in combination with either method Vd1/CL1 (Fig. 5A) or method Vd2/CL2 (Fig. 5B). Method Vd1/CL1 was a poor predictor of V_d/F in that only 5 predictions were within 2-fold of observed (22%, Fig. 5A), with bias toward overprediction (*afe*) and poor precision (*rmse*) (Table 4). In contrast, method Vd2/CL2 resulted in more accurate predictions of V_d/F with 16 compounds within 2-fold of observed (70%, Fig. 5B). Although this method showed slight bias toward underprediction, the bias and precision were better than those obtained with

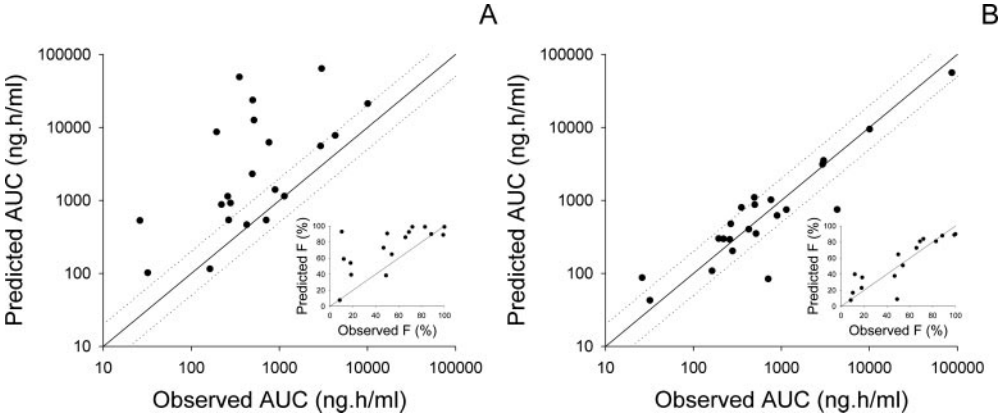

FIG. 4. Prediction accuracy for the physiologically based predictions of human area under the plasma concentration-time curve after oral dosing (AUC) and absolute oral bioavailability (*F*, insets) obtained using the ACAT model and method CL1 (A), and the ACAT model and method CL2 (B). For more details on all methods used, refer to *Materials and Methods*. Lines signify unity and 2-fold errors between predicted and experimentally determined parameters.

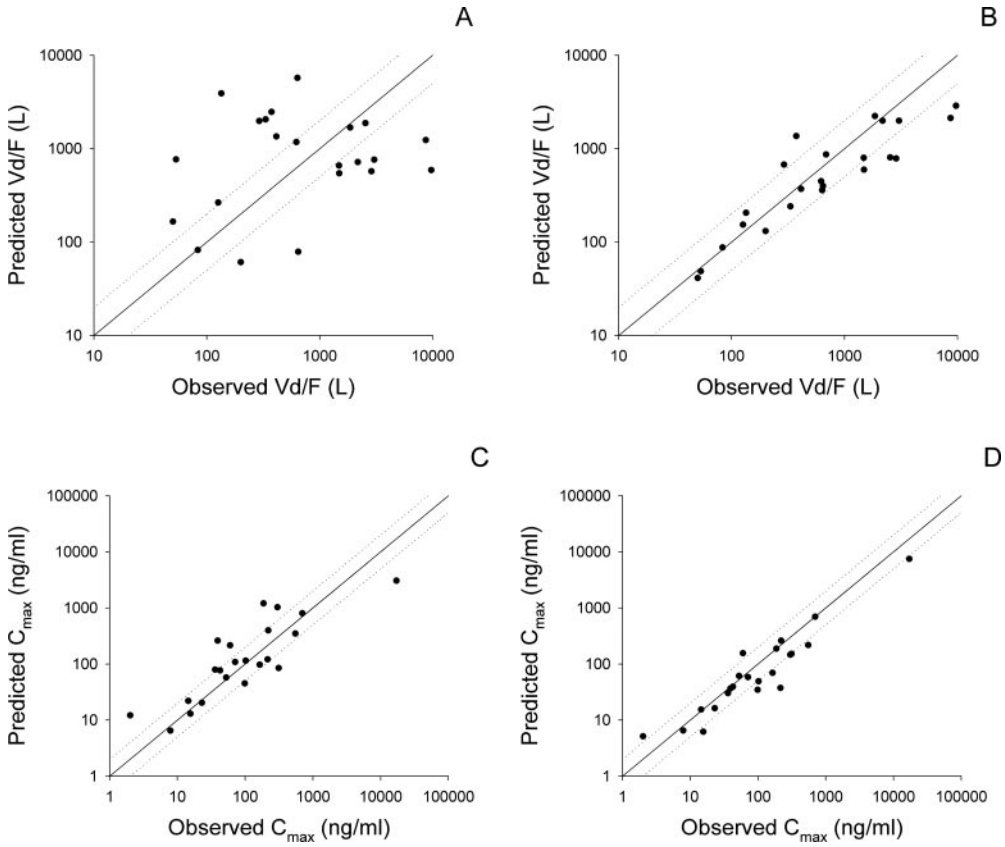

FIG. 5. A and B, prediction accuracy for the physiologically based predictions of the apparent volume of distribution after oral administration (V_d/F) obtained using the ACAT model and method Vd1/CL1(A) or the ACAT model and method Vd2/CL2 (B). C and D, prediction accuracy for the physiologically based predictions of the peak plasma concentration after oral dosing (C_{max}) obtained using the ACAT model and method Vd1/CL1 (C) or the ACAT model and method Vd2/CL2 (D). For more details on all methods used, refer to *Materials and Methods*. Lines signify unity and 2-fold errors between predicted and experimentally determined parameters.

method Vd1/CL1 as indicated by the decreased *afe* and *rmse* values (Tables 4 and 5).

The correlations between the observed and predicted C_{max} using the ACAT model in combination with either method Vd1/CL1 or method Vd2/CL2 are presented in Fig. 5, C and D, respectively. Both methods had similar accuracy to predict C_{max} (Tables 4 and 5).

Prediction Accuracy of Oral Plasma Concentrations. There were 23 compounds that had suitable data for assessment of oral plasma concentrations. In Fig. 6, the simulated plasma concentration-time profiles using the ACAT model in combination with either method Vd1/CL1 (Fig. 6, solid line) or method Vd2/CL2 (Fig. 6, dotted line) are shown, together with the observed data (Fig. 6, open squares). In general, method Vd2/CL2 yielded the best agreement between the mean observed and predicted plasma values, as indicated by the *afe* and *rmse* values (Table 8).

Discussion

The use of whole-body PBPK modeling is becoming more popular within the pharmaceutical industry. This is due to a combination of estimating the PK characteristics of compounds as early as possible, with making efficient and informed selection on which compounds to progress (van de Waterbeemd and Gifford, 2003; Jones et al., 2006a). The development of mechanism-based prediction tools for the assessment of P_{tp} and CL_H based on in vitro data has greatly contributed to the early applications of PBPK modeling (Theil et al., 2003). Although these prediction tools show great promise, it has been recognized that inaccurate predictions will occur if the underlying assumptions of the mechanistic equations are not met (Parrott et al., 2005b; Jones et al., 2006a). Therefore, more studies are required to assess how the prediction accuracy as well as the type of data needed will vary depending on the approach, the type of chemistry, and the prediction system used. To the best of our knowledge, the current study represents the first attempt to explore how an integrated use of both experimental and predicted data can improve PK predictions using whole-body PBPK modeling. A dataset of 26 compounds formed the reference data in our study. It is acknowledged that the number of compounds might be below the optimum to draw general conclusions about the usefulness of the approaches investigated; nevertheless, it is still large enough to show some clear trends.

The present evaluation indicates that the type of tissue distribution data used must be carefully considered. The most accurate approach toward prediction of human V_{ss} considered a combined set of predicted and experimental in vivo rat P_{tp} data (84% within 2-fold, method Vd2), whereas predictions based on physicochemical input alone were rather poor (32% within 2-fold, method Vd1). This finding illustrates that V_{ss} predictions can be improved by considering limited experimental in vivo rat P_{tp} data (Table 2). Experimental P_{tp} data must, however, be carefully selected since V_{ss} is largely determined by P_{tp} of adipose and muscle tissues (Bjorkman, 2002), which were available for most of the compounds (Table 2). A second clear trend was that correction of rat P_{tp} data for interspecies differences in plasma protein binding yielded better predictions compared with when binding differences were ignored (84% versus 53% within 2-fold). This observation was anticipated because in scaling tissue distribution from rat to human, the unbound human P_{tp} values are generally assumed to be identical to those of rat (Sawada et al., 1984). Nevertheless, in the case of basic drugs, the accuracy of this assumption remains uncertain since electrostatic interactions with acidic phospholipids have been identified as a major factor controlling tissue distribution (Rodgers et al., 2005b), and an interspecies variability in the acidic phospholipids has been indicated (Rodgers et al., 2005a).

Mechanistic equations to predict tissue distribution from physicochemical input have been developed by Poulin and Theil (Pou-

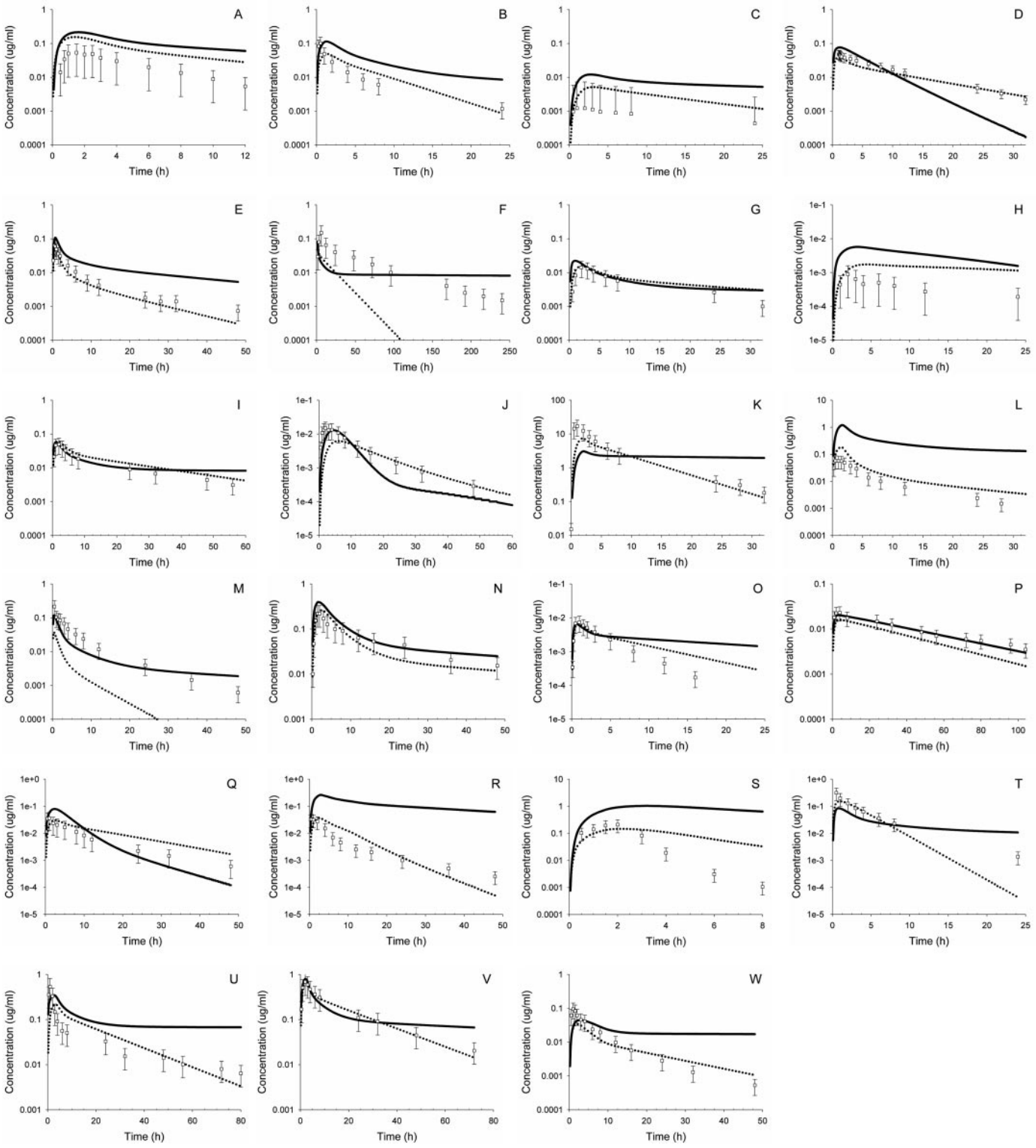

FIG. 6. Predictions of human plasma concentration-time profiles after oral dosing using the ACAT model and either method Vd1/CL1 (dotted line) or Method Vd2/CL2 (solid line) for: A, JNJ1; B, JNJ2; C, JNJ3; D, JNJ4; E, JNJ7; F, JNJ8; G, JNJ9; H, JNJ10; I, JNJ11; J, JNJ12; K, JNJ13; L, JNJ14; M, JNJ15; N, JNJ16; O, JNJ18; P, JNJ19; Q, JNJ20; R, JNJ21; S, JNJ22; T, JNJ23; U, JNJ24; V, JNJ25; and W, JNJ26. The observed data are shown in open squares. For more details on all methods used, refer to *Materials and Methods*.

lin and Theil, 2000, 2002; Poulin et al., 2001), who reported that for a set of 123 drugs, 80% of the predicted V_{ss} values were within 2-fold of observed. In the current study, the overall prediction accuracy using these equations was reduced to 42% and 32% within 2-fold of observed for rat and human, respectively. A decreased prediction accuracy of these equations was also observed by others (Parrott et al., 2005a; Jones et al., 2006a). This may be explained by distribution processes that are not covered in these equations, such as active transport or ionic interactions of charged bases with acidic phospholipids of cell membranes. In the

TABLE 8

Statistics for the predicted human plasma concentrations after oral dosing

For details on prediction of oral plasma concentrations using method Vd1/CL1 and method Vd2/CL2, see *Materials and Methods*.

Approach	n^a	*afe*	*rmse*	Percentage within 1.5-fold Error	Percentage within 2-fold Error	Percentage within 3-fold Error
Method Vd1/CL1	261	2.29	1.57	25.7	36.5	50.9
Method Vd2/CL2	261	1.03	1.20	43.4	60.0	74.8

[a] The total pool ($n = 261$) of mean plasma concentrations (ug/ml) for all compounds of TABLE 2 after oral dosing.

Poulin and Theil (2002) equation, ionic interactions are not included and tissue binding is extrapolated from plasma protein binding. We have shown that using this approach, tissue binding of bases is prone to underestimation, particularly for strong bases that have low plasma protein binding such as JNJ4, JNJ10, and JNJ20 (De Buck et al., 2007). In this study, however, the V_{ss} of most compounds was overpredicted, despite the fact that they were bases (Fig. 2A). Although this finding may be explained by a limitation in membrane permeation, this explanation seems rather unlikely given the overall high permeability of the compounds within our dataset. Another explanation may be a consistent overprediction of P_{tp} values of adipose tissue, which is a major contributor to the total V_{ss}. For example, V_{ss} prediction can be easily biased by the investigator's choice on the RA value for adipose tissue (eqs. 1 and 2). In this study and those by others, it has been assumed that the RA value for adipose tissue equals 0.15 (Jones et al., 2006a). However, in the original work of Poulin and Theil (2002), the RA value for adipose tissue was assumed to be 0. Future work will assess whether an optimization of the RA value based on the outcome of the prediction in rat may improve prediction accuracy.

The decision of whether to incorporate blood binding (fu_p/R_B) and in vitro incubation matrix binding (fu_{inc}) in CL_H predictions remains controversial (Obach, 1999; Riley et al., 2005; De Buck et al., 2007). The inclusion of both unbound fractions has been suggested as the generally acceptable approach. However, our results and those by others demonstrate that in the case of some compound classes, especially basic ones, disregarding all binding values may yield the most accurate predictions (method CL2, 74% within 2-fold) (Obach, 1997, 1999; De Buck et al., 2007), whereas inclusion of both correction factors yielded large underpredictions (method CL1, 53% within 2-fold). It is acknowledged, however, that underpredictions (Fig. 2C) may prevail because the contribution of extrahepatic metabolism and biliary clearance to CL has been neglected; therefore, scaled microsomal or hepatocyte data may not always be able to fully project CL. To the best of our knowledge, oxidative microsomal metabolism was the major route of elimination for the compounds within this study. Despite these uncertainties, our findings obtained in human were in agreement with those obtained in rat, suggesting that an assessment of the prediction accuracy in rat could be used to guide which approach is most likely to succeed. For renally cleared compounds (JNJ4, JNJ12, JNJ19, JNJ20), the empirical GFR approach successfully extrapolated human CL_R from rat data. This is in agreement with previous reports that have achieved good predictions of CL_R using this approach (Lin, 1998; Jones et al., 2006a).

The ability to successfully predict a drug's dosing regimen by predicting human in vivo $t_{1/2}$ is of tremendous value in the compound selection process. The most accurate prediction of in vivo $t_{1/2}$ was obtained using method Vd2/CL2 (69% within 2-fold). In contrast, in vivo $t_{1/2}$ prediction was strongly biased toward overprediction using a combination of methods Vd1 and CL1, most probably as a result of overprediction of V_{ss} and underprediction of CL, respectively (Table 4). These results indicate that accurate predictions of both V_{ss} and CL are critical in the prediction of in vivo $t_{1/2}$.

In the prediction of oral AUC, both the CL and fraction of oral dose absorbed are important. As expected, the most accurate predictions of AUC were obtained using the most accurate input on CL (method CL2). For the purpose of this study, intestinal wall metabolism was ignored, yet the prediction of oral absorption parameters was on the whole quiet successful, suggesting that the contribution of intestinal metabolism may be low. It is acknowledged that this represents a shortcoming, and ideally its contribution should be considered. Estimates of fraction of oral dose absorbed were obtained using the ACAT model and were based on the drug's in vitro input on permeability and solubility. Unfortunately, in this dataset there were only two BCS class III compounds (high solubility and low permeability) for which the limiting effect of permeability could be assessed (JNJ10, JNJ12). For such compounds, accurate estimates of permeability are imperative for successful predictions. In this study, converted Caco-2 permeability data provided accurate predictions, whereas inaccurate predictions were observed using in silico predicted counterparts (data not shown). The vast majority of the compounds were highly permeable and belong to either BCS class I (high solubility) or BCS class II (low solubility). For BCS class II compounds, the outcome of simulations may be sensitive to the nature and accuracy of the solubility input. Aqueous solubility data may not reflect actual solubility in vivo, resulting in a strong bias toward underprediction of bioavailability (Parrott et al., 2005b; Jones et al., 2006a). For two compounds that were practically insoluble in aqueous media (JNJ21, JNJ24), solubility measurements in SIF were found to provide a good alternative.

Prediction of V_d/F and C_{max} rely on the rate of absorption as well as the methods used for prediction of CL and V_{ss}. The ACAT model may serve as a time-dependent input function of PBPK disposition models and thus allows prediction of full plasma concentration-time profiles. As expected, the most accurate prediction of V_d/F was obtained using method Vd2/CL2 (70% within 2-fold), whereas prediction was strongly biased toward overprediction using method Vd1/CL1 (21% within 2-fold). In contrast, prediction of C_{max} (65% within 2-fold) was less sensitive to the choice of methods used for prediction of V_{ss} and CL. This may be explained by time-dependent prediction errors, which are usually more pronounced on terminal plasma concentrations (Fig. 6).

In summary, these results and those by others demonstrate that a generic physiologically based prediction approach can lead to reasonable predictions of human pharmacokinetics (Jones et al., 2006a,b). However, the prediction accuracy may vary depending on the approach, and significant mis-predictions can occur when the underlying assumptions of the model or prediction tool are not met. PBPK model validation on each of the key input parameters using in vitro assays in

combination with preclinical data remains the recommended strategy for human PBPK modeling.

Acknowledgments. We thank the many colleagues at Johnson & Johnson Pharmaceutical Research and Development (Beerse, Belgium) who have generated data used in these analyses, with a special thanks to everybody who currently supports the in vitro and in vivo pharmacokinetic studies and bioanalytical assays.

References

Agoram B, Woltosz WS, and Bolger MB (2001) Predicting the impact of physiological and biochemical processes on oral drug bioavailability. *Adv Drug Deliv Rev* **50 (Suppl 1):**S41–S67.

Austin RP, Barton P, Cockroft SL, Wenlock MC, and Riley RJ (2002) The influence of nonspecific microsomal binding on apparent intrinsic clearance, and its prediction from physicochemical properties. *Drug Metab Dispos* **30:**1497–1503.

Bischoff KB (1986) Physiological pharmacokinetics. *Bull Math Biol* **48:**309–322.

Bjorkman S (2002) Prediction of the volume of distribution of a drug: which tissue-plasma partition coefficients are needed. *J Pharm Pharmacol* **54:**1237–1245.

De Buck SS, Sinha VK, Fenu LA, Gilissen RA, Mackie CE, and Nijsen MJ (2007) The prediction of drug metabolism, tissue distribution, and bioavailability of 50 structurally diverse compounds in rat using mechanism-based absorption, distribution, and metabolism prediction tools. *Drug Metab Dispos* **35:**649–659.

Ellmerer M, Schaupp L, Brunner GA, Sendlhofer G, Wutte A, Wach P, and Pieber TR (2000) Measurement of interstitial albumin in human skeletal muscle and adipose tissue by open-flow microperfusion. *Am J Physiol Endocrinol Metab* **278:**E352–E356.

Giuliano C, Jairaj M, Zafiu CM, and Laufer R (2005) Direct determination of unbound intrinsic drug clearance in the microsomal stability assay. *Drug Metab Dispos* **33:**1319–1324.

Houston JB (1994) Utility of in vitro drug metabolism data in predicting in vivo metabolic clearance. *Biochem Pharmacol* **47:**1469–1479.

Houston JB and Carlile DJ (1997) Prediction of hepatic clearance from microsomes, hepatocytes, and liver slices. *Drug Metab Rev* **29:**891–922.

Ito K and Houston JB (2004) Comparison of the use of liver models for predicting drug clearance using in vitro kinetic data from hepatic microsomes and isolated hepatocytes. *Pharmacol Res* **21:**785–792.

Ito K and Houston JB (2005) Prediction of human drug clearance from in vitro and preclinical data using physiologically based and empirical approaches. *Pharmacol Res* **22:**103–112.

Iwatsubo T, Hirota N, Ooie T, Suzuki H, Shimada N, Chiba K, Ishizaki T, Green CE, Tyson CA, and Sugiyama Y (1997) Prediction of in vivo drug metabolism in the human liver from in vitro metabolism data. *Pharmacol Ther* **73:**147–171.

Iwatsubo T, Hirota N, Ooie T, Suzuki H, and Sugiyama Y (1996) Prediction of in vivo drug disposition from in vitro data based on physiological pharmacokinetics. *Biopharm Drug Dispos* **17:**273–310.

Jones HM, Parrott N, Jorga K, and Lave T (2006a) A novel strategy for physiologically based predictions of human pharmacokinetics. *Clin Pharmacokinet* **45:**511–542.

Jones HM, Parrott N, Ohlenbusch G, and Lave T (2006b) Predicting pharmacokinetic food effects using biorelevant solubility media and physiologically based modelling. *Clin Pharmacokinet* **45:**1213–1226.

Kantharaj E, Tuytelaars A, Proost PE, Ongel Z, Van Assouw HP, and Gilissen RA (2003) Simultaneous measurement of drug metabolic stability and identification of metabolites using ion-trap mass spectrometry. *Rapid Commun Mass Spectrom* **17:**2661–2668.

Leo A, Hansch C, and Elkins D (1971) Partition coefficients and their uses. *Chem Rev* **71:**525–615.

Lin JH (1998) Applications and limitations of interspecies scaling and in vitro extrapolation in pharmacokinetics. *Drug Metab Dispos* **26:**1202–1212.

Obach RS (1997) Nonspecific binding to microsomes: impact on scale-up of in vitro intrinsic clearance to hepatic clearance as assessed through examination of warfarin, imipramine, and propranolol. *Drug Metab Dispos* **25:**1359–1369.

Obach RS (1999) Prediction of human clearance of twenty-nine drugs from hepatic microsomal intrinsic clearance data: an examination of in vitro half-life approach and nonspecific binding to microsomes. *Drug Metab Dispos* **27:**1350–1359.

Obach RS, Baxter JG, Liston TE, Silber BM, Jones BC, MacIntyre F, Rance DJ, and Wastall P (1997) The prediction of human pharmacokinetic parameters from preclinical and in vitro metabolism data. *J Pharmacol Exp Ther* **283:**46–58.

Parrott N, Jones H, Paquereau N, and Lave T (2005a) Application of full physiological models for pharmaceutical drug candidate selection and extrapolation of pharmacokinetics to man. *Basic Clin Pharmacol Toxicol* **96:**193–199.

Parrott N, Paquereau N, Coassolo P, and Lave T (2005b) An evaluation of the utility of physiologically based models of pharmacokinetics in early drug discovery. *J Pharm Sci* **94:**2327–2343. 16136543 Year does not match (2005).

Pelkonen O, Kaltiala EH, Larmi TK, and Karki NT (1973) Comparison of activities of drug-metabolizing enzymes in human fetal and adult livers. *Clin Pharmacol Ther* **14:**840–846.

Poulin P, Schoenlein K, and Theil FP (2001) Prediction of adipose tissue: plasma partition coefficients for structurally unrelated drugs. *J Pharm Sci* **90:**436–447.

Poulin P and Theil FP (2000) A priori prediction of tissue:plasma partition coefficients of drugs to facilitate the use of physiologically-based pharmacokinetic models in drug discovery. *J Pharm Sci* **89:**16–35.

Poulin P and Theil FP (2002) Prediction of pharmacokinetics prior to in vivo studies. 1. Mechanism-based prediction of volume of distribution. *J Pharm Sci* **91:**129–156.

Riley RJ, McGinnity DF, and Austin RP (2005) A unified model for predicting human hepatic, metabolic clearance from in vitro intrinsic clearance data in hepatocytes and microsomes. *Drug Metab Dispos* **33:**1304–1311.

Rodgers T, Leahy D, and Rowland M (2005a) Physiologically based pharmacokinetic modeling 1: predicting the tissue distribution of moderate-to-strong bases. *J Pharm Sci* **94:**1259–1276.

Rodgers T, Leahy D, and Rowland M (2005b) Tissue distribution of basic drugs: accounting for enantiomeric, compound and regional differences amongst beta-blocking drugs in rat. *J Pharm Sci* **94:**1237–1248.

Rodgers T and Rowland M (2006) Physiologically based pharmacokinetic modelling 2: predicting the tissue distribution of acids, very weak bases, neutrals and zwitterions. *J Pharm Sci* **95:**1238–1257.

Sawada Y, Hanano M, Sugiyama Y, Harashima H, and Iga T (1984) Prediction of the volumes of distribution of basic drugs in humans based on data from animals. *J Pharmacokinet Biopharm* **12:**587–596.

Sun D, Lennernas H, Welage LS, Barnett JL, Landowski CP, Foster D, Fleisher D, Lee KD, and Amidon GL (2002) Comparison of human duodenum and Caco-2 gene expression profiles for 12,000 gene sequences tags and correlation with permeability of 26 drugs. *Pharmacol Res* **19:**1400–1416.

Theil FP, Guentert TW, Haddad S, and Poulin P (2003) Utility of physiologically based pharmacokinetic models to drug development and rational drug discovery candidate selection. *Toxicol Lett* **138:**29–49.

Ungell AL, Nylander S, Bergstrand S, Sjoberg A, and Lennernas H (1998) Membrane transport of drugs in different regions of the intestinal tract of the rat. *J Pharm Sci* **87:**360–366.

van de Waterbeemd H and Gifford E (2003) ADMET in silico modelling: towards prediction paradise? *Nat Rev Drug Discov* **2:**192–204.

Willmann S, Schmitt W, Keldenich J, Lippert J, and Dressman JB (2004) A physiological model for the estimation of the fraction dose absorbed in humans. *J Med Chem* **47:**4022–4031.

Yu LX and Amidon GL (1999) A compartmental absorption and transit model for estimating oral drug absorption. *Int J Pharm* **186:**119–125.

Address correspondence to: Stefan S. De Buck, Ablynx nv, Technologiepark 4, B-9052 Ghent/Zwijnaarde, Belgium. E-mail: stefan.debuck@ablynx.com